

# Low-Frequency Loudspeaker Assessment by Nearfield Sound-Pressure Measurement\*

D. B. KEELE, JR.

*Electro-Voice, Inc., Buchanan, Mich. 49107*

A loudspeaker test technique is described which depends on nearfield pressure measurements made in a nonanechoic environment. The technique allows extremely simple measurements to be made of frequency response, power response, distortion, and electroacoustical efficiency.

## GLOSSARY OF SYMBOLS

$a$	radius of circular radiator
$a_D$	radius of diaphragm, $= \sqrt{S_D/\pi}$
$a_V$	radius of circular vent, $= \sqrt{S_V/\pi}$
$c$	velocity of sound in air, $= 343$ m/s
$e_{in}$	voltage applied to driver input
$f$	frequency, in Hz
$f_B$	Helmholtz resonance frequency of vented box
$f_3$	low-frequency cutoff ( $-3$ dB) of speaker system
$I_o$	acoustic intensity, in power per unit area, $= p^2/(2 \rho_o c)$ for a plane wave
$k$	wave number, $= 2\pi/\lambda = \omega/c$
$p$	peak sound pressure
$p_F$	peak sound pressure in farfield of acoustic radiator
$p_N$	peak sound pressure in nearfield of acoustic radiator
$p_{N_{rms}}$	root mean square sound pressure in nearfield of radiator, $= p_N/\sqrt{2}$
$p_R$	peak sound pressure on axis of piston at distance $r$
$P_A$	acoustic output power
$P_E$	nominal electrical input power
$Q$	ratio of reactance to resistance (series circuit) or resistance to reactance (parallel circuit)
$Q_B$	$Q$ or cabinet at $f_B$ considering all system losses

$r$	distance from pressure sample point to center of piston
$R_E$	dc resistance of driver voice coil
$S$	surface area
$S_D$	effective projected surface area of driver diaphragm
$S_V$	cross-sectional area of vent
SPL	sound pressure level, in dB re $20 \mu$ N/m <sup>2</sup>
$U_o$	output volume velocity of acoustic radiator
$\lambda$	wavelength of sound in air, $= c/f$
$\eta$	nominal power transfer efficiency, $= P_A/P_E$
$\eta_o$	reference efficiency defined for radiation into a half-space free field
$\rho_o$	density of air, $= 1.21$ kg/m <sup>3</sup> at 20° C
$\omega$	radian frequency variable, $= 2 \pi f$ .

**INTRODUCTION:** The low-frequency evaluation of a loudspeaker system with respect to frequency response, distortion, and power output has traditionally required the use of a large and expensive anechoic chamber or a cumbersome and often equally costly open-field outdoor testing site. Recently, Small [1] pointed out that valid measurements could be made at very low frequencies in any reasonable environment by sampling the pressure inside the enclosure.<sup>1</sup>

<sup>1</sup> Even the large anechoic chamber at Electro-Voice is not much good for low-frequency measurements below 40 Hz in the farfield (beyond 10 ft (3 m) from the speaker system being tested). EV engineers have resorted to Small's technique numerous times to measure response below this frequency.

\* Presented May 15, 1973, at the 45th Convention of the Audio Engineering Society, Los Angeles.

This paper describes a very simple measurement method which is based on measurements taken in the nearfield outside the enclosure and, like Small's method, may be used in any environment. However, this method does not require the frequency-dependent signal processing circuitry of Small's method and is accurate over a wider frequency range.

## THEORY

### Pressure on Axis

Consider a rigid flat circular piston mounted in an infinite flat baffle (half-space) generating peak sinusoidal acoustic volume velocity  $U_o$  (Fig. 1). The nearfield and

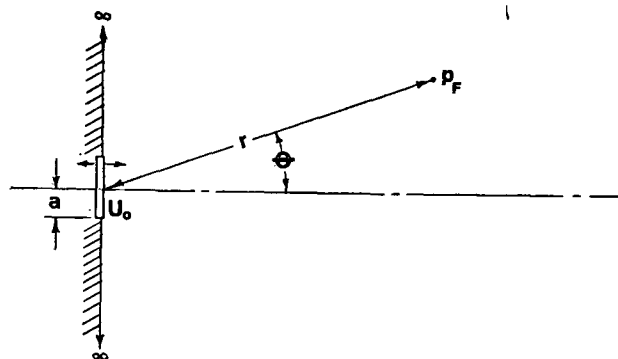


Fig. 1. Rigid circular piston of radius  $a$  radiating into a half-space freefield ( $2\pi$  sr). The piston vibrates with peak volume velocity  $U_o$  and generates peak farfield pressure  $p_F$  at distance  $r$  away from center of piston.

farfield sound pressures for this case can be derived from the following equation, which gives the pressure magnitude along the piston axis for measurement distances  $r$  varying over the complete range of zero to infinity [2, p. 175]:

$$p_R = \frac{2\rho_o c U_o}{\pi a^2} \cdot \sin \left[ \frac{k}{2} \left( \sqrt{r^2 + a^2} - r \right) \right] \quad (1)$$

where

- $p_R$  peak pressure magnitude measured at distance  $r$  from piston
- $a$  piston radius
- $c$  velocity of sound in air, = 343 m/s
- $k$  wave number, =  $2\pi/\lambda = \omega/c$
- $r$  distance from measuring point to center of piston
- $U_o$  piston peak output volume velocity
- $\rho_o$  density of air, = 1.21 kg/m<sup>3</sup> at 20° C.

### Farfield Pressure

At points far from the piston where  $r \gg a$  and for low frequencies such that  $ka < 1$ , Eq. (1) can be shown to converge to

$$p_F = \frac{\rho_o c k U_o}{2\pi r} \quad (2)$$

where  $p_F$  is the peak axial pressure measured at distance  $r$  in the farfield of the piston. This relationship of course is the familiar equation that gives the farfield low-frequency sound pressure for any generalized simple sound source of

strength  $U_o$  radiating from an infinite baffle [2, Eq. (7.40), p. 165]. Eq. (2) exhibits the well-known inverse relationship between pressure and distance.

### Nearfield Pressure

At points very close to the center of the piston where  $r \ll a$ , Eq. (1) gives

$$p_N = p_R(r=0) = \frac{2\rho_o c U_o}{\pi a^2} \cdot \sin \left( \frac{ka}{2} \right) \quad (3)$$

where  $p_N$  is the peak pressure in the nearfield at the center of the piston. If the frequency is low enough such that  $ka < 1$ , Eq. (3) reduces to

$$p_N = \frac{\rho_o c k U_o}{\pi a} \quad (4)$$

Fig. 2 shows a plot of Eq. (3) divided by  $\rho_o c k U_o / (\pi a)$  as a function of  $ka/(2\pi) = a/\lambda$ . This plot represents the normalized frequency dependence of the pressure in the nearfield of a rigid piston operating in the constant acceleration mode. The pressure is found to be constant up to the frequency where  $a/\lambda = 0.26$  ( $ka = 1.6$ ), the pressure fall being just 1 dB at this frequency. For frequencies such that the piston radius is a wavelength or multiple of a wavelength ( $a = n\lambda$  for  $n = 1, 2, 3, \dots$ ), nulls are found to exist because of interference effects. For frequencies above  $a/\lambda = 0.5$  ( $ka > \pi$ ) the pressure envelope falls at 6 dB per octave.

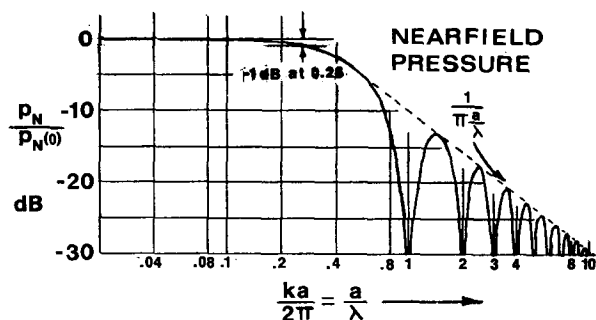


Fig. 2. Frequency dependence of nearfield sound pressure at points close to center of a rigid circular piston operating in a constant accelerating mode (mass-controlled region). Nearfield pressure nulls are found to exist whenever the piston's radius is equal to a wavelength or integral multiple thereof.

### Near-Far Pressure Relationships

Dividing Eq. (4) by Eq. (2) and solving for  $p_N$  yields

$$p_N = \frac{2r}{a} \cdot p_F \quad (5)$$

This surprising result shows that for low frequencies ( $ka < 1$ ) the nearfield sound pressure is directly proportional to the farfield sound pressure. The relationship depends only on the ratio of the piston radius to the farfield sample distance and is independent of frequency. From a practical measurement standpoint, the nearfield sound pressure  $p_N$  and volume velocity  $U_o$  are essentially independent of the environment into which the piston is radiating [1, p. 29]. This means that valid inferences can be made about the low-frequency farfield anechoic operation

of a particular speaker system from nonanechoic measurements of the nearfield sound pressure.

A parallel derivation for the case of a piston radiating into a full space at low frequencies yields

$$p_N = \frac{4r}{a} \cdot p_P \tag{6}$$

### Measuring Distance

To investigate more fully the axial sound pressure dependence on measuring distance, Eq. (1) is examined in more detail. For distances from the piston less than  $0.75 a^2/\lambda$ , plane waves are radiated which are contained essentially within a cylinder of diameter  $2a$  [3, p. 187]. For distances beyond  $2a^2/\lambda$  approximately spherical divergence is found to hold, where the pressure falls inversely as the distance. For frequencies equal to or higher than the frequency where  $a = \lambda$  ( $ka \geq 2$ ), the pressure is found to go through a series of maxima with intervening nulls as the distance from the piston's surface is increased. For low frequencies such that  $ka < 2\pi$  the only pressure null occurs at  $r = \infty$ . A plot of Eq. (1), normalized to the maximum axial pressure for several values of  $a/\lambda$ , is in Fig. 3.

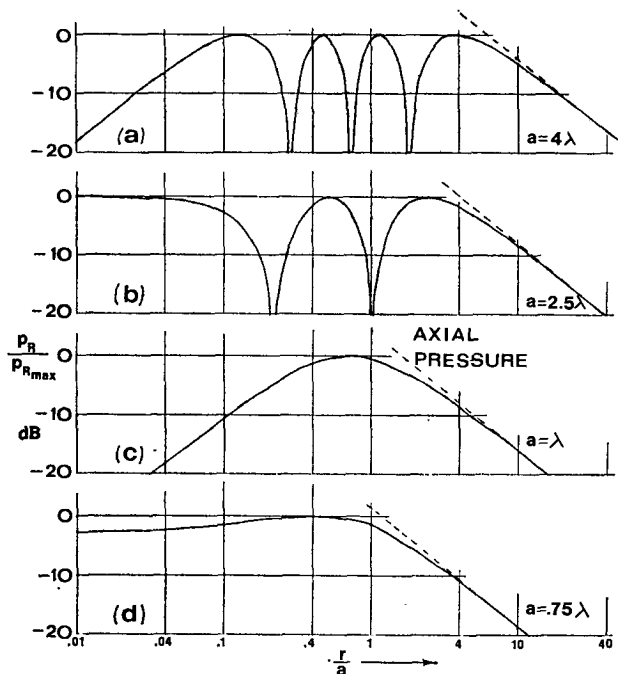


Fig. 3. Sound pressure along axis of a rigid circular piston radiating into a half-space freefield for several values of  $a/\lambda$ .

If the upper frequency of measurement is limited such that  $ka < 1$ , a division of Eq. (1) by Eq. (4) with the substitution  $\sin X \approx X$  yields:

$$\frac{p_R}{p_N} = \frac{\sqrt{r^2 + a^2} - r}{a} = \sqrt{\left(\frac{r}{a}\right)^2 + 1} - \frac{r}{a} \tag{7}$$

Eq. (7) gives the low-frequency axial dependence of pressure on measuring distance normalized to the nearfield pressure occurring at  $r = 0$ . A plot of Eq. (7) on a dB versus  $\log(r/a)$  scale is shown in Fig. 4. To be within 1 dB of the true nearfield pressure, the measuring pressure microphone must be no farther away from the center sur-

face of the piston than  $0.11a$ . For low frequencies, farfield conditions exist for distances beyond  $2a$ .

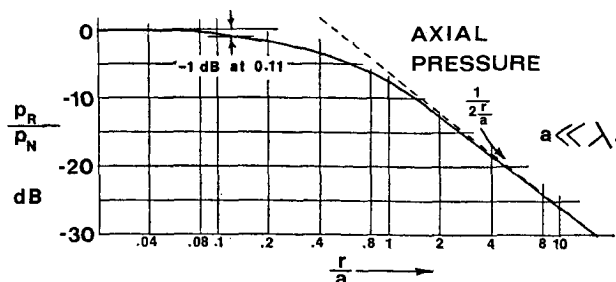


Fig. 4. Sound pressure along axis of a rigid circular piston radiating into a half-space freefield, for frequencies low enough such that  $ka < 1$  (loudspeaker piston range).

### Flat Piston Pressure Distribution

The analysis so far has considered only measurement points near the center and along the axis of a flat circular piston. In general, the nearfield sound pressure distribution over the surface of a piston is very complicated, especially for the higher frequencies ( $ka > 2\pi$ ). Zemanek [3], in an excellent numerical analysis, presents the fine details of the nearfield pressure distribution for a circular piston operated in this higher frequency range.

Fortunately, in the low-frequency piston range of operation ( $ka < 1$ ) the nearfield pressure is very well behaved and smoothly distributed. For  $ka \leq 2$ , McLachlan [4, p. 49] has evaluated the exact expression for the pressure distribution at the surface of a rigid circular piston. Fig. 5, which shows the radial dependence of pressure magnitude for  $ka = 0.5$  and 2, displays some of McLachlan's work. Examination of Fig. 5 reveals that the low-frequency nearfield pressure varies quite gradually as a function of surface position reaching a maximum at the piston center.

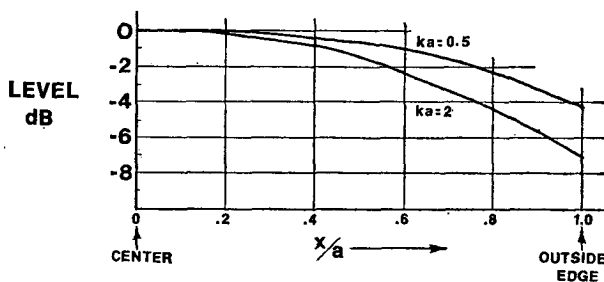


Fig. 5. Normalized nearfield sound pressure distribution on surface of a rigid circular piston vibrating in an infinite flat baffle, for  $ka = 0.5$  and 2. The distribution exhibits circular symmetry and is only a function of the radial distance from the center to the edge of the piston (after [4]).

### Conical Piston Pressure Distribution

The diaphragms of real world loudspeakers are usually constructed in the form of truncated right circular cones. The crucial question in this study is whether flat circular piston theory can be extended to measurements on conical pistons.

The author is unaware of any documented studies of the nearfield sound distribution of a vibrating cone and cannot give a definite answer to the question posed above. However, nearfield measurements made on a number of

direct-radiator cone speaker systems have correlated extremely well with measurements made by other conventional means. In every case the nearfield sample was taken where the nearfield pressure was at a maximum, i.e., usually at a point near the cone's apex or speaker's dust dome.

**Radiated Sound Power**

The total radiated sound power output of an arbitrary acoustic source radiating into a half-space is found by integrating the intensity function over a hemisphere enclosing the source. If the radius of the hemisphere is large

substitution of  $p_N = \sqrt{2} p_{N_{rms}}$  yielding

$$P_A = \frac{S_D}{2 \rho_0 c} \cdot p_{N_{rms}}^2 \tag{10}$$

This equation indicates that for the low-frequency piston range operation of the radiator ( $ka < 1$ ), the total radiated sound power may be assessed by a simple measurement of the nearfield sound pressure at the center of the piston. Fig. 6 plots this relationship for acoustic power output in watts versus  $p_{N_{rms}}$  in dB re  $20 \mu\text{N/m}^2$  for several values of piston size.

**Efficiency**

The power conversion efficiency of the transducer is given by the ratio of the acoustic output power to nominal electrical input power for radiation into a specified environment (taken here as half space or  $2 \pi$  sr). For the specific case of a loudspeaker driver with voice coil dc resistance  $R_E$ , the nominal electrical input power  $P_E$  is defined as the power available across  $R_E$  for applied source voltage  $e_{in}$  [5, p. 386]:

$$P_E = e_{in}^2 / R_E \tag{11}$$

The efficiency may be computed in terms of the nearfield pressure and input voltage by dividing Eq. (10) by Eq. (11), giving

$$\eta = \frac{P_A}{P_E} = \frac{S_D R_E}{2 \rho_0 c} \cdot \frac{p_{N_{rms}}^2}{e_{in}^2} \tag{12}$$

This relationship yields efficiencies that are within 1 dB of the true efficiency for  $ka < 1.6$  (assuming the piston operates rigidly in this region). Fig. 7 plots this relationship for the specific situation of 1 volt rms applied to a driver whose  $R_E$  is 10 ohms, for several values of piston size. For other values of  $R_E$ , the values of  $\eta$  obtained from this figure can be scaled accordingly (if  $R_E$  is higher or lower than 10 ohms the efficiency is higher or lower in direct proportion). An efficiency curve has been included in Fig. 7 for a piston of 10 in<sup>2</sup> (64.5 cm<sup>2</sup>) true effective area to ease computations of efficiency for radiators of other sizes. Thus the efficiency of any driver is the value given by this curve multiplied by the ratio of actual piston area to 10 in<sup>2</sup> (64.5 cm<sup>2</sup>) and again by the ratio of actual voice-coil resistance to 10 ohms.

**Frequency and Power Response**

As stated earlier, Eq. (5) indicates that the relationship between near and far sound pressures depends only on two length constants and is independent of frequency (for  $ka < 1$ ). Therefore, low-frequency response can be measured quite simply by plotting the nearfield pressure (in dB) versus frequency. Total acoustic power output versus frequency can then be derived using Eq. (10) or Fig. 6.

**Distortion**

Because of relation (5), completely valid measurements of low-frequency harmonic distortion can be made in the nearfield and these should correlate well with an identical set of measurements in the farfield if all distortion components are within the specified frequency limit. Somewhat lower nearfield distortion values are to be expected

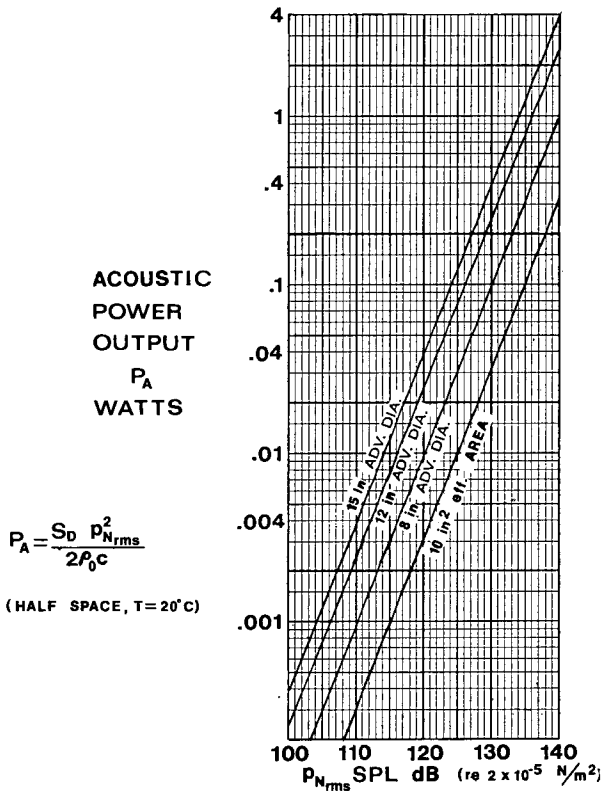


Fig. 6. Total radiated sound power  $P_A$  of a rigid circular piston radiating into a half-space to nearfield sound pressure level measured at points close to center of piston, for low frequencies such that  $ka < 1$ . The following piston sizes are plotted: 10-in<sup>2</sup> (64.5-cm<sup>2</sup>) effective (actual) area, 8-in (20.3-cm) advertised diameter (6.2-in (15.7-cm) effective diameter), 12-in (30.5-cm) advertised diameter (9.8-in (26.9-cm) effective diameter), and 15-in (38-cm) advertised diameter (12.6-in (32-cm) effective diameter).

enough so that all points on the hemisphere are in the farfield of the source, and if the source is radiating essentially omnidirectionally ( $ka < 1$ ), the radiated acoustic power is given by

$$P_A = \int \int_{S_0} I_0 dS = \frac{\pi r^2}{\rho_0 c} \cdot p_F^2 \tag{8}$$

Solving Eq. (5) for  $p_F$  and substitution into Eq. (8) yields

$$P_A = \frac{\pi a^2}{4 \rho_0 c} \cdot p_N^2 = \frac{S_D}{4 \rho_0 c} \cdot p_N^2 \tag{9}$$

where  $S_D$  is the effective area of the piston.

Eq. (9) may be rewritten for the case of rms pressure by

where distortion harmonics exceed this limit. The relatively high SPL found in the nearfield of a piston can actually aid distortion measurements because the acoustic signal-to-noise ratio is much improved. In most cases, meaningful distortion tests can be made even in a noisy laboratory environment.

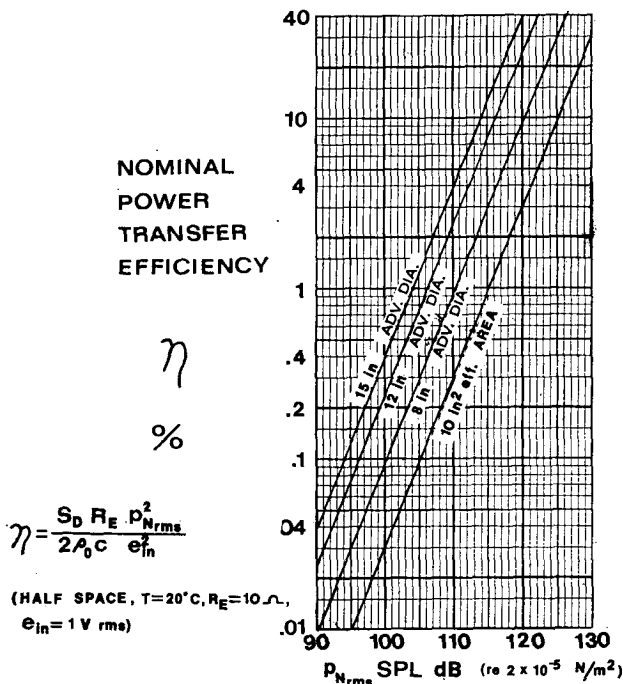


Fig. 7. Relationship between nominal efficiency of a loudspeaker driver operating as a rigid piston and radiating into a half-space and nearfield sound pressure level, for frequencies low enough such that  $ka < 1$ . The graph is normalized to unit input voltage ( $e_{in} = 1\ \text{V rms}$ ) and voice coil resistance  $R_E$  of 10 ohms. Refer to Fig. 6 for description of piston sizes.

### LOUDSPEAKER SYSTEM MEASUREMENTS

The nearfield pressure measurement technique is a very powerful tool for evaluating the performance of assembled loudspeaker systems. A nearfield pressure frequency response measurement of each driver in a system (both in and out of the system) can answer a whole host of questions concerning low-frequency bass response, overall system frequency response, system efficiency, relative efficiency, and levels between drivers, distortion, etc.

#### Closed Box

The woofer's nearfield pressure frequency response, measured with constant known drive voltage, is a direct analogue of the frequency response that would be measured in an anechoic chamber (half-space loading) for the piston range of operation. Figs. 6 and 7 can be used in this case to plot system acoustic power output and efficiency as a function of frequency (knowing  $e_{in}$ ,  $R_E$ , and resultant nearfield SPL).

In-box measurements of nearfield SPL can be taken of all the drivers in a multiway system with crossover connected to provide data for computation of relative levels, approximate overall frequency response, efficiencies, and crossover frequencies. Eq. (5) can be used to compute each individual driver's contribution to the farfield pres-

sure. Assuming roughly equal individual driver directional characteristics and equal farfield pressure contributions (equal efficiencies), the nearfield SPL is found to be inversely proportional to the linear dimensions of each driver (i.e., the tweeter, which is the smallest, has the highest nearfield SPL).

#### Vented Box

The nearfield pressure technique is found to work well for measurement of the low-frequency characteristics of the vented enclosure system. The complete system operation for a multiway vented-box system can be assessed in the same manner as the closed-box system by measuring the nearfield pressure of each driver individually. The following comments apply to the piston-range operation of the woofer mounted in the vented enclosure.

The vented-box system frequency response can be evaluated using the nearfield method. Benson [6, p. 47] displays the theoretical overall low-frequency response of a 4th-order Butterworth (Thiele's alignment no. 5 [7]) vented system, along with the individual contributions of the vent and driver. Fig. 8 is a reproduction of these data.

The driver diaphragm response is found to exhibit a null at the vented-box resonance frequency  $f_B$ . The depth of the null is found to be directly related to the total cabinet losses  $Q_B$  [8, p. 414]. A simple measurement of the driver nearfield SPL frequency response reveals the value of  $f_B$  by noting the frequency of the null. The driver reference efficiency  $\eta_0$  can be derived (with the aid of Fig. 7) by noting the nearfield SPL in the level response region above  $2f_B$  with 1 volt rms applied.

The vent's contribution to the total system output can be likewise determined by a nearfield response measurement of the vent. For best results, the measurement microphone should be placed in the center of the vent, flush with the front surface of the cabinet. Practical measurements of the vent nearfield output in the frequency range above  $f_B$  reveal that the measured response is contaminated by crosstalk from the diaphragm. Valid nearfield SPL measurements of the vent can only be made for frequencies less than about  $1.6f_B$ .

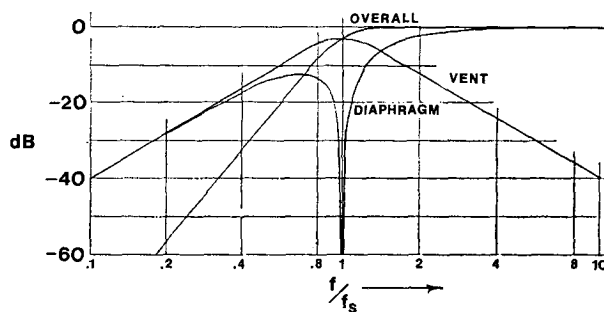


Fig. 8. Theoretical sound pressure frequency response of a vented undamped-enclosure loudspeaker system aligned so that the overall response conforms to a 4th-order Butterworth high-pass filter function (Thiele alignment no. 5 [7]). Individual farfield pressure responses are shown for the contributions of vent and diaphragm (after [6]).

The individually measured nearfield responses of the vent and driver may be used to construct an approximate farfield overall system frequency response. Eq. 5 must again be used to adjust the relative levels of diaphragm and vent, according to their respective diameters, before

the responses can be summed. For example, if the vent diameter is one half the effective diameter of the driver diaphragm, the driver output must be increased by 6 dB before the outputs can be summed. The summation implied here is of course vectorial, where both magnitude and phase must be considered. It is noted, however, that the port and cone are roughly in phase above  $f_B$  and out of phase below  $f_B$  (for high cabinet  $Q$ ). At  $f_B$  the system output is predominantly that of the vent. For situations where crosstalk is not much of a problem, one might even perform the indicated summation by using two microphones (one for the diaphragm and one for the vent) and then combining the microphone outputs by the use of a microphone mixer with input gains set appropriately.

**EXPERIMENTAL MEASUREMENTS**

Measurements were taken experimentally on several different types of systems to verify the theory and techniques put forth in this paper. A list of the measuring equipment used, along with a brief explanation of how Small's box-pressure measurement method [1] was implemented, is outlined in the Appendix.

**SPL and Frequency Response Versus Distance**

Eqs. (5), (7), and Fig. 4 were checked by making experimental measurements in the anechoic chamber on a 4½-in (11.4-cm) (1½-in (3.8-cm) effective piston radius) full-range driver in a closed box, flush mounted in the center of an 8- by 4-ft (2.4- by 1.2-m) baffle board (roughly a half-space for distances not far from the board). The 395-in³ (6473-cm³) closed test box was roughly cubical, with external dimensions of 7.75 by 8.25 by 8.5 in (19 by 21 by 21.7 cm). The driver was mounted from the outside, off center, on the 8.25- by 8.5-in (21- by 21.7-cm) face.

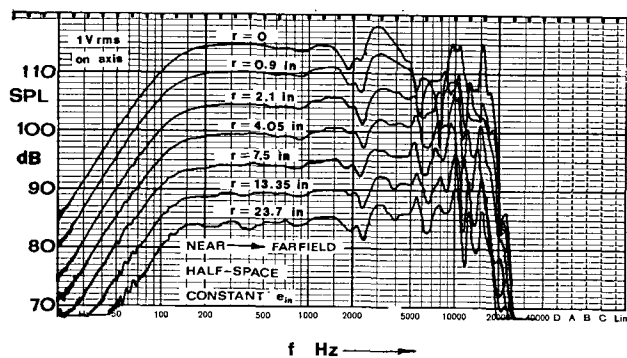


Fig. 9. Experimental measurements performed to check Eq. (7) and Fig. 4. The source is a 4.5-in (11.4-cm) wide-range driver, mounted in a 395-in³ (6473-cm³) closed box, flush mounted in the center of a 4- by 8-ft (1.2- by 2.4-m) sheet of ¾-in (1.9-cm) plywood. Seven anechoic axial frequency response measurements were made with the measurement microphone the indicated distance from the diaphragm. The distances chosen correspond to low-frequency axial attenuations of 0, -5, -10, -15, -20, -25, and -30 dB relative to the nearfield pressure at  $r = 0$ .

Several axial constant-voltage frequency responses were taken at different distances from the driver, extending from the nearfield ( $r < 0.11a$ ) into the farfield ( $r > 5a$  for low frequencies). Distances corresponding to low-frequency axial attenuations of 0, -5, -10, -15, -20,

-25, and -30 dB (referred to nearfield pressure) were chosen ( $r = 0, 0.6a, 1.4a, 2.7a, 5a, 8.9a,$  and  $15.8a$ , from Fig. 4). Fig. 9 shows the results of these measurements. The figure indicates close agreement with theory for all frequencies less than about 2 kHz ( $ka \approx 1.4$ ). Note the large variation in signal-to-noise ratio between the responses in Fig. 9 and the improvement gained in the nearfield ( $r = 0$ ).

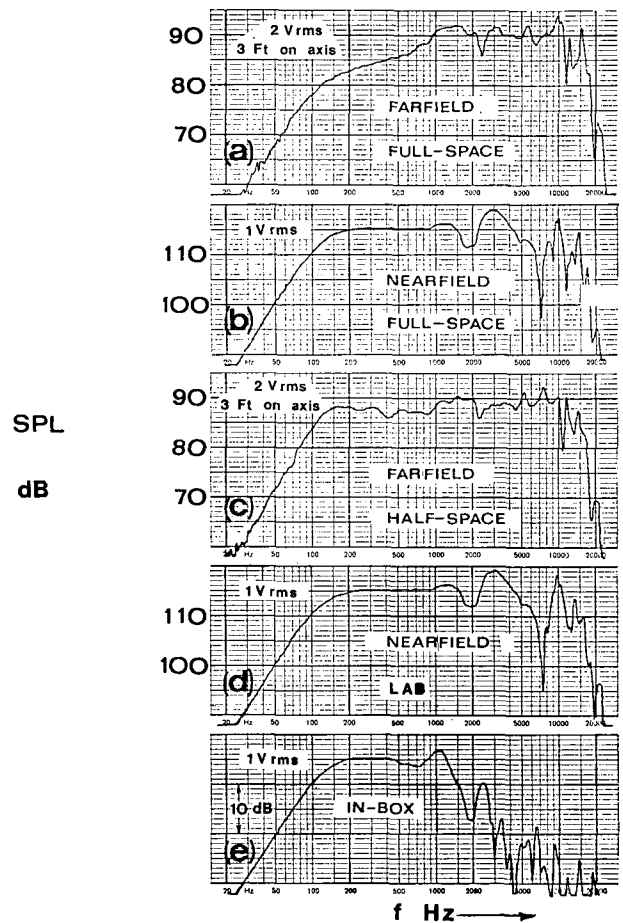


Fig. 10. Experimental frequency response measurements on the 4.5-in (11.4-cm) closed-box system of Fig. 9. The response was measured five different ways. a. In anechoic chamber in farfield ( $4 \pi$  sr). b. In anechoic chamber in driver's nearfield ( $4 \pi$  sr). c. On a 4- by 8-ft (1.2- by 2.4-m) baffle board, in chamber, in farfield ( $2 \pi$  sr). d. In lab on floor, in nearfield. e. In box using the method of Small [1].

**Frequency Response Measured by Different Methods**

The axial frequency response of the 4½-in (11.4-cm) closed-box system, described in the previous section, was measured using several different methods: 1) in the anechoic chamber in the driver's farfield (full space), 2) in the anechoic chamber in the driver's nearfield (full space), 3) in the anechoic chamber mounted on the 4- by 8-ft (1.2- by 2.4-m) baffle board in the driver's farfield (half-space), 4) in the laboratory sitting on the test bench in the driver's nearfield, and 5) inside the test box enclosure using Small's box-pressure measurement method [1]. These test results are displayed in Fig. 10.

Note the differences between the farfield responses of Fig. 10a and c that were measured in the  $4 \pi$  and  $2 \pi$  environments. Diffraction effects and increasing cabinet

directivity with frequency causes a rising characteristic in the response from about 100 to 800 Hz in the  $4\pi$  space [9], [10].

Keeping in mind the expected differences between Fig. 10a and c, the frequency responses measured by the five methods show good agreement below 500 Hz. A comparison between the two indirect methods (Fig. 10d, e) reveals that the nearfield technique yields accurate response data about  $1\frac{1}{2}$  octaves higher than the box-pressure technique.

### System Measurements

To illustrate system measurements with the nearfield technique, two loudspeaker systems were measured, an 8-in (20.3-cm) two-way closed-box acoustic suspension system and a 15-in (38.1-cm) three-way vented-box system.

#### Closed-Box

The closed-box direct-radiator system consisted of an 8-in (20.3-cm) diameter (6.2-in (15.7-cm) effective piston diameter) high-compliance woofer, and a  $2\frac{1}{2}$ -in (6.4-cm) diameter (2-in (5-cm) effective diameter) closed-back tweeter.

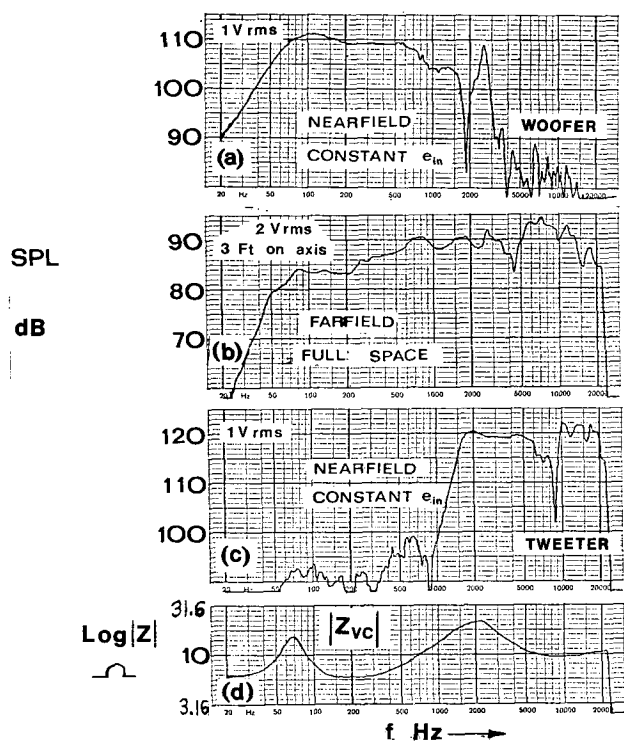


Fig. 11. Experimental measurements made on an 8-in (20.3-cm) woofer 2.5-in (6.3-cm) tweeter, two-way acoustic-suspension closed-box system. a. Nearfield frequency response of woofer (crossover connected for all these tests) with constant applied voltage. b. Frequency response in anechoic chamber in farfield ( $4\pi$  sr). c. Nearfield response of tweeter with 1 volt rms applied. d. System driving-point impedance magnitude versus frequency.

Nearfield frequency responses were run on both drivers in this system with a constant system input voltage of 1 volt rms. The tests were run with the drivers mounted in the enclosure, in their correct positions, with the system crossover connected. An anechoic chamber free-field (full-space) response was measured for comparison. These responses are shown in Fig. 11.

The nearfield measurement of the tweeter (Fig. 11c) shows that its nearfield SPL is roughly 10 dB higher than that of the woofer. This level difference is expected because the tweeter is roughly one third the diameter of the woofer (assuming equal farfield SPL for each driver operating in the piston range). The measured voice-coil resistance  $R_B$  of the woofer is 4.8 ohms, and the calculated efficiency for the level portion of the system low-frequency piston range (200–500 Hz) is 0.35%.

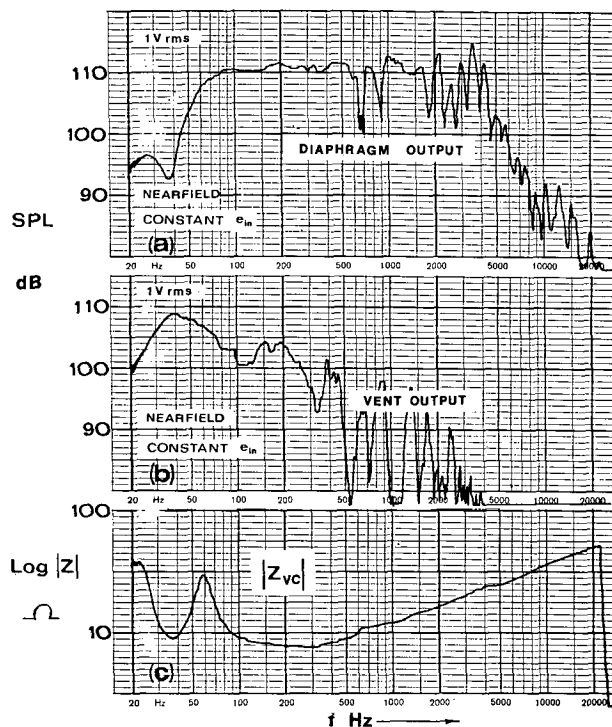


Fig. 12. Display of experimental measurements taken on 15-in (38.1-cm) vented-box system theoretically set up for a 4th-order Butterworth response with a corner ( $-3$  dB) frequency of 40 Hz. a. Nearfield pressure frequency response at center of driver's diaphragm. b. At center of vent. c. Woofer's driving point impedance magnitude versus frequency.

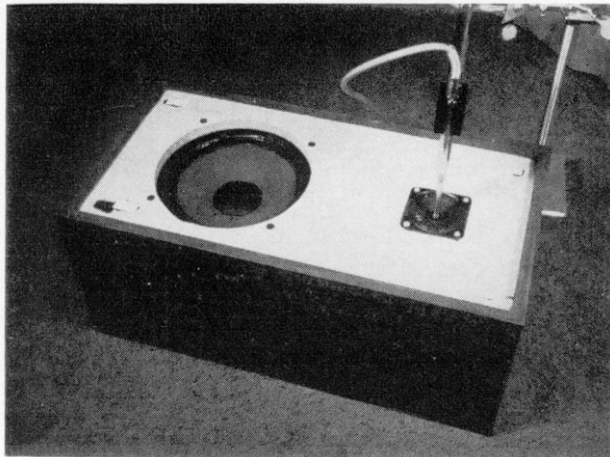
#### Vented-Box

The measurements on the vented enclosure system were limited to the woofer section only. The three-way 15-in (38.1-cm) vented-box system consists of a direct-radiator vented-box low end with horn-loaded midrange and tweeter. The low end of this system is designed to have a 4th-order Butterworth high-pass response (Thiele alignment no. 5) with  $f_B = f_3 = 40$  Hz. The driver's effective piston diameter is 13 in (33 cm) [ $S_D = 133$  in<sup>2</sup> (858 cm<sup>2</sup>)], the vent size is 7 by  $10\frac{3}{4}$  in (17.8 by 27.3 cm) [ $S_V = 75$  in<sup>2</sup> (484 cm<sup>2</sup>)], and the net internal box volume  $V_B$  is 6.3 ft<sup>3</sup> (0.18 m<sup>3</sup>). The voice-coil dc resistance  $R_B$  is 6.5 ohms.

The nearfield SPL measurements on this system are shown in Fig. 12 along with an impedance curve. The vent measurement was taken with the test microphone held in the center of the vent flush with the enclosure's outside surface (for valid vent measurements, the system drive voltage must be low enough to ensure sinusoidal air movement and low turbulence at the vent output). Fig. 13 displays photographs of the nearfield measurements being taken on this system.

The driver diaphragm output (Fig. 12a) shows good correspondence with the theoretical curve displayed in

Fig. 8. The vent output (Fig. 12b) shows the effects of diaphragm crosstalk above 80 Hz when compared to Fig. 8.



a



b



c

Fig. 13. Nearfield measurements on assorted direct radiators in nonanechoic environment. a. Tweeter in 8-in (20.3-cm) two-way closed-box system (1/4-in (0.6-cm) microphone). b. Woofer in 15-in (38.1-cm) vented-box system. c. Vent in 15-in (38.1-cm) vented-box system.

An approximate overall low-frequency response was derived from these data by first computing the relative size ratio between vent and driver diaphragm:

$$\frac{a_D}{a_V} = \sqrt{\frac{S_D}{S_V}} = \sqrt{\frac{133}{75}} = 1.33.$$

This value corresponds to a farfield pressure level shift of about +2.5 dB in favor of the diaphragm (for equal nearfield SPL, the diaphragm would contribute 2.5 dB more level to the farfield pressure because of its larger size).

Examination of the nearfield responses for vent and cone (Fig. 12a and b) reveals that the vent output at box resonance (about 38 Hz) is down approximately 2 dB from the diaphragm's output in the level response region extending from 100 to 500 Hz. The total system output is therefore down about 4.5 dB at 38 Hz. This single-point output computation at  $f_B$ , coupled with the knowledge that the vented-box system rolls off at 24 dB per octave below  $f_B$ , was used with the measured cone output response (Fig. 12a) to derive the approximate low-frequency response in Fig. 14 ( $f_3 \approx 41$  Hz). The efficiency in level portion of the piston-range response, from Fig. 7, is 3.1%.

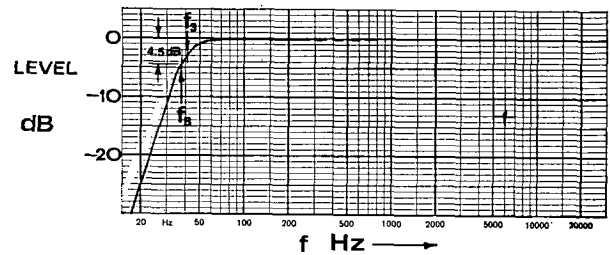


Fig. 14. Approximate overall low-frequency response of 15-in (38.1-cm) vented-box system derived from measurements made using nearfield pressure sampling technique (Fig. 12). The response indicates that system is slightly mistuned from a 4th-order Butterworth alignment at 40 Hz because the box resonance frequency  $f_B$  is somewhat low.

### CONCLUSION

The theory presented, along with supporting experimental measurements, shows that loudspeaker system piston-range characteristics can easily be measured by sampling the nearfield pressure with a test microphone held close to the acoustic radiator. Valid nearfield measurements may be taken in any reasonable environment without the use of an anechoic chamber or large outdoor test site. Experimental measurements using the nearfield technique show excellent agreement with more traditional test methods.

### APPENDIX

#### Experimental Measuring Equipment

The following equipment was used in making the measurements presented in this paper.

- 1) Beat frequency audio oscillator, Bruel and Kjaer (B&K) type 1014.
- 2) Power amplifier, 200 watt, McIntosh, model MI-200AB.
- 3) Capacitor microphone, 1/4 in, B&K type 4135 with follower.
- 4) Capacitor microphone, 1/2 in, B&K type 4133 with follower.
- 5) Precision measurement amplifier, B&K type 2606.
- 6) Graphic level recorder, B&K type 2305.



### Implementation of Box-Pressure Measurements

The frequency equalization network used to implement Small's box-pressure measurement method [1] was corrected only for the  $1/\omega^2$  behavior [1, p. 29, eq. (2) and (3)] of the box pressure. Box compliance shift and enclosure loss effects were not compensated for. A second-order high-pass RC filter, with corner frequency of 1 kHz ( $-3$  dB), was used to provide an approximate  $\omega^2$  response up to about 1 kHz for these measurements.

### ACKNOWLEDGMENT

The author is indebted to Raymond J. Newman, Senior Engineer, Loudspeaker Systems, at Electro-Voice, for first making the observation that nearfield measurements correlated well with anechoic measurements. (When the author first joined Electro-Voice in June 1972, Ray had been making frequency response measurements using this method for about a year.)

The criticism and review of this manuscript by John Gilliom, Chief Product Engineer, Loudspeakers, at EV, and Ray Newman is gratefully acknowledged. The author is further indebted to Dr. Richard H. Small of the University of Sydney, Australia, for comments, suggested revisions, and constructive criticisms of this paper.

### REFERENCES

- [1] R. H. Small, "Simplified Loudspeaker Measure-

ments at Low Frequencies," *J. Audio Eng. Soc.*, vol. 20, pp. 28-33 (Jan./Feb. 1972).

[2] L. E. Kinsler and A. R. Frey, *Fundamentals of Acoustics* (Wiley, New York, 1962).

[3] J. Zemanek, "Beam Behavior Within the Nearfield of a Vibrating Piston," *J. Acoust. Soc. Am.*, vol. 49, pp. 181-191 (1971).

[4] N. W. McLachlan, *Loudspeaker Theory, Performance, Testing and Design* (Publications, New York, 1960).

[5] R. H. Small, "Direct-Radiator Loudspeaker System Analysis," *J. Audio Eng. Soc.*, vol. 20, pp. 383-395 (June 1972).

[6] J. E. Benson, "Theory and Design of Loudspeaker Enclosures Part I: Electro-Acoustical Relations and Generalized Analysis," *Amalgamated Wireless (Australasia) Ltd. Tech. Rev.*, vol. 14, pp. 1-57 (Aug. 1968).

[7] A. N. Thiele, "Loudspeakers in Vented Boxes," *J. Audio Eng. Soc.*, vol. 19, pp. 382-392 (May 1971); pp. 471-483 (June 1971).

[8] J. E. Benson, "Theory and Design of Loudspeaker Enclosures Part III: Introduction to Synthesis of Vented Systems," *A.W.A. Tech. Rev.*, vol. 14, pp. 369-484 (Nov. 1972).

[9] H. F. Olson, "Direct Radiator Loudspeaker Enclosures," *J. Audio Eng. Soc.*, vol. 17, pp. 22-29 (Jan. 1969).

[10] R. F. Allison and R. Berkovitz, "The Sound Field in Home Listening Rooms," *J. Audio Eng. Soc.*, vol. 20, pp. 459-469 (July/Aug. 1972).

---

**Note:** Mr. Keele's biography appears in the January/February 1973 issue of the Journal.